Ultrafast photoexcited cyclotron emission: Contributions from real and virtual excitations

Daniel Some* and Arto V. Nurmikko
Brown University, Department of Physics and Center for Advanced Material Research, Box M, Providence, Rhode Island 02912
(Received 19 October 1995; revised manuscript received 25 March 1996)

The coherent cyclotron transients generated upon femtosecond interband photoexcitation of GaAs are studied under different magnetic-field configurations. By varying the excitation wavelength, we are able to discriminate between contributions to the THz emission due to ballistic transport and instantaneous inter-Landau-level polarizations. [S0163-1829(96)51920-X]

The terahertz (THz) transients radiated upon ultrafast photoexcitation of semiconductor surfaces at ambient conditions have been well characterized,[1–5] demonstrating the role of the surface depletion field E_s as well as the crystalline symmetry in the primary mechanisms in the emission process: (a) ballistic acceleration of photocarriers, (b) instantaneous polarization of electron-hole pairs, and (c) bulk $\chi^{(2)}$ rectification. In the case of above-bandgap excitation of [100] GaAs at low intensities, only the first two of these are important, and are directly related to the presence of the surface field; besides providing the potential drop for ballistic acceleration, E_s serves to break the symmetries which would otherwise cause the total nonlinear polarization due to spatially nonlocal pair creation to vanish. Virtual excitations created by sub-bandgap illumination have also been demonstrated to produce THz pulses,[6] directly illustrating the optical rectification effect attributable to the depletion field. Hu *et al.*[7] time resolved the screening effect of the real and virtual excitations created by one laser pulse on the THz transient produced by a second pulse with 10-fsec resolution, identifying the instantaneous polarization and ballistic transport processes through their temporal dependencies.

In an earlier publication[8] we reported the coherent ultrafast cyclotron transients produced in photoexcited [100] GaAs subject to a magnetic field and low temperature, as detected via standard THz optoelectronic time-domain techniques. In this paper we extend the previous work: by investigating the effect of varying the photon excitation energy, we are able to distinguish between the contributions of real and virtual excitations to the transient cyclotron signal. Two experimental configurations are employed, as described in Fig. 1. The configuration shown in Fig. 1(a), denoted ''tilted Faraday'' (TF), is identical to that of Ref. 8. The normal to the sample surface is tilted at $\theta = 25°$ with respect to the magnetic field in order that there be a component of E_s perpendicular to B, which is necessary in order to activate the Lorentz force $\mathbf{F} = \mathbf{q}(\mathbf{E} + \boldsymbol{v} \times \mathbf{B})$. The Voigt configuration depicted in Fig. 1(b) sets the magnetic field in the plane of the sample and thus perpendicular to E_s. The output of a 100-MHz mode-locked Ti:sapphire laser, composed of 70-fsec pulses and wavelength tunable in the range of $\lambda = 740–850$ nm, was split into two parts; 150–200 mW of average power was used to excite the samples, typically at a temperature of 5 K, over an area on the order of 1 cm^2, and the second portion of the beam was used to gate a photoconductive, ion-damaged silicon-on-sapphire-based antenna. By sweeping the delay of the gating pulse with respect to the exciting pulse, one time resolves the electric field emitted by the sample with sub-picosecond accuracy. The frequency response of our antenna was calibrated against a bolometer-based interferometer.

One aspect of the physics underlying the two configurations, which pertains to our goal of discriminating between cyclotron emission due to ballistic motion of charges versus coherent inter-Landau-level polarizations, may be conveniently illustrated through the classical solution of the trajectory of a charged particle subject to oblique electric and magnetic fields separated by an angle θ: $\mathbf{E} = E \sin\theta \hat{\mathbf{x}} + E \cos\theta \hat{\mathbf{z}}$ and $\mathbf{B} = B\hat{\mathbf{z}}$. Assuming that the particle of mass m and charge q begins at rest, its velocity will evolve as

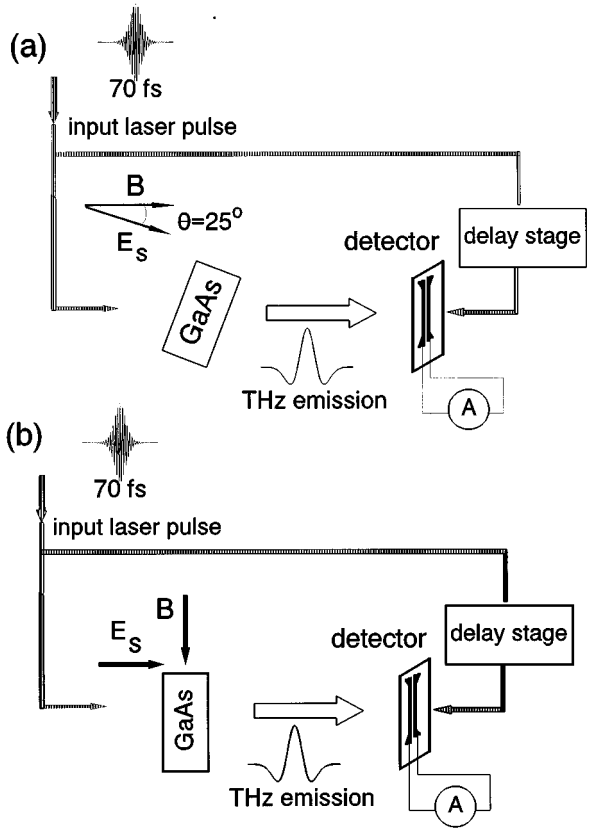

FIG. 1. The experimental layout and magnetic-field geometries employed in these experiments: (a) TF and (b) Voigt.

$$v_x(t) = \pm (E \sin\theta/B)\ \sin\omega_c t,$$

$$v_y(t) = \pm (E \sin\theta/B)\,(1 - \cos\omega_c t), \qquad (1)$$

$$v_z(t) = (qtE \cos\theta/m)\,,$$

where $\omega_c = eB/m$ and the signs of v_x and v_y depend on the sign of q. If the two fields are perpendicular, then $v_z = 0$ and the total kinetic energy is bounded (note that particles elastically scattered into finite z-momentum states will still not undergo acceleration, and their average v_z will vanish); for typical values of $E_s = 1$–5 kV/cm and $B = 2$ T the kinetic energy is on the order of a few meV. This value is well below the longitudinal-optical (LO) phonon energy in GaAs ($\hbar\omega_{\mathrm{LO}} = 37$ meV), so no dephasing via LO-phonon emission is expected. However, at our value of θ in the TF geometry of Fig. 1(a), a free electron will attain kinetic energy along $\hat{z}$ equal to that of one LO-phonon within 0.2–0.5 psec. This time scale is typical of LO-phonon emission events by hot electrons in bulk GaAs, and may also be compared with the 70-fsec intervalley scattering time identified by Hu *et al.* in biased *p-i-n* structures.[7] Hence an electron streaming along the direction of the magnetic field (while simultaneously executing circular cyclotron motion around the B-field line) can be expected to undergo several scattering events within the time scale of a cyclotron orbit (1–2 psec in our field range), making the possibility of coherent cyclotron emission from an ensemble of such particles rather unlikely.

Such is not the case if the THz signal is due to coherent, transient inter-Landau-level polarizations, as would be produced in the presence of the depletion field by spatially nonvertical transitions. Assuming a crystal of cubic symmetry, it is clear from the separability of the Hamiltonian for a particle in the magnetic and electric fields described above

$$H = H_\perp + H_\parallel,$$

$$H_\perp = \frac{1}{2m}[(p_x - \tfrac{1}{2}By)^2 + (p_y + \tfrac{1}{2}Bx)^2] + qEx\cos\,\theta, \quad (2)$$

$$H_\parallel = \frac{1}{2m}p_z^2 + qEz\ \sin\theta,$$

that the intraband polarization parallel to B is decoupled from the polarization perpendicular to B. The coherent induced polarizations will dephase via the usual processes at work in low temperature, such as scattering from impurities or interfaces, but not via the inelastic phonon-emission process.

Two additional electron-phonon phenomena which must be considered in the context of differentiating between processes involving ''real'' and ''virtual'' excitations are the magnetophonon resonance and the magnetopolaron effect. As argued below, the Frölich interaction leads to a resonant magnetopolaron state, producing different effective cyclotron masses for real and virtual excitations in the vicinity of the resonance. On the other hand, we find quite contrasting behavior for the two radiative mechanisms near the magnetophonon resonance: at the appropriate excitation energy, an LO-phonon-mediated energy and phase relaxation of a *real* carrier may take place between the nth and $n = 0$ Landau levels, while *virtual* excitations do not undergo this relaxation. Gubarev *et al.*[9] have found that magnetoluminescence (i.e., recombination of ''real'' electrons and light holes) in bulk GaAs is nearly completely quenched at $\hbar\omega \approx 1.59$ eV $\approx E_g + 2\hbar\omega_{\mathrm{LO}}$, indicating that the carriers have rapidly relaxed via phonon emission (we note that, due to the similar masses of the electron and light hole, approximately $2\hbar\omega_{\mathrm{LO}}$ is required for the electron to have $1\hbar\omega_{\mathrm{LO}}$ of excess energy). This differentiation between phase relaxation processes of real and virtual excitations is analogous to that of hot-exciton luminescence and resonant Raman scattering in polar semiconductors: real carriers (i.e., ''hot'' excitons) dephase via inelastic LO-phonon scattering, whereas the virtual excitations (i.e., Raman polarizations) retain phase coherence despite their strong coupling to the phonons.[10]

We focus here on experimental results obtained at magnetic fields of 1.5 and 2.0 T in both the TF and Voigt geometries, and for the range of photon excitation energies of 1.51–1.68 eV stepped by 20 meV (due to the bandwidth of the transform-limited 70-fsec laser pulses). These B-field values are convenient in that the electron cyclotron frequency is in the vicinity of the peak response of our THz photoconductive detector. The time-domain data was Fourier transformed into amplitude spectra in the frequency domain and normalized by the system response; examples are shown in Figs. 2(a) and 2(b). Figure 2(c) plots the integrated spectral amplitude of the emission as a function of excitation energy, where the TF data (indicated by square symbols) has been magnified by a factor of 2.5 in order to account for the $\sin\theta$ term in (1). While all of the curves are seen to initially rise as the excitation energy shifts through the band gap at 1.52 eV, the TF amplitude remains nearly constant at higher energies. On the other hand, the Voigt data (circle symbols) exhibit a large dip in the range of $\hbar\omega = 1.59$–1.61 eV, on the order of 30% of the peak value, suggesting the onset of the electron-light-hole magnetophonon resonance at roughly $E_g + 2\hbar\omega_{\mathrm{LO}}$. Note that, at the bottom of the dip, the Voigt amplitude is nearly equal to the TF amplitude. We also find in the Voigt data evidence for a second dip at the high-energy side of the spectrum. However, the point where a two-phonon resonance might be expected at ~ 1.68 eV is beyond the tuning range of our laser.

Cyclotron electron effective masses were extracted using $m^* = eB/\omega_c$ from the spectra by fitting to the sum of several Lorenzian peaks, representing electron and light- and heavy-hole resonances together with a broad ''continuum'' which appears below the highest frequency (i.e., electron resonance) peak. While not addressing this feature here any further, the continuum may be ascribed to a variety of virtual inter-valence-band transitions which are no longer dipole forbidden, due to symmetry breaking by the surface depletion field. Figures 3(a) and 3(b) plot the experimental electron masses, as derived from the fits, against photon energy; the nonparabolic conduction-band structure of GaAs is apparent in the increase of mass with excitation energy. More intriguing is the peak at $\hbar\omega \sim 1.61$ eV for the Voigt configuration [Fig. 3(b)], which is more pronounced at the higher B field; whereas in the TF data [Fig. 3(a)] the effective mass rather levels off.

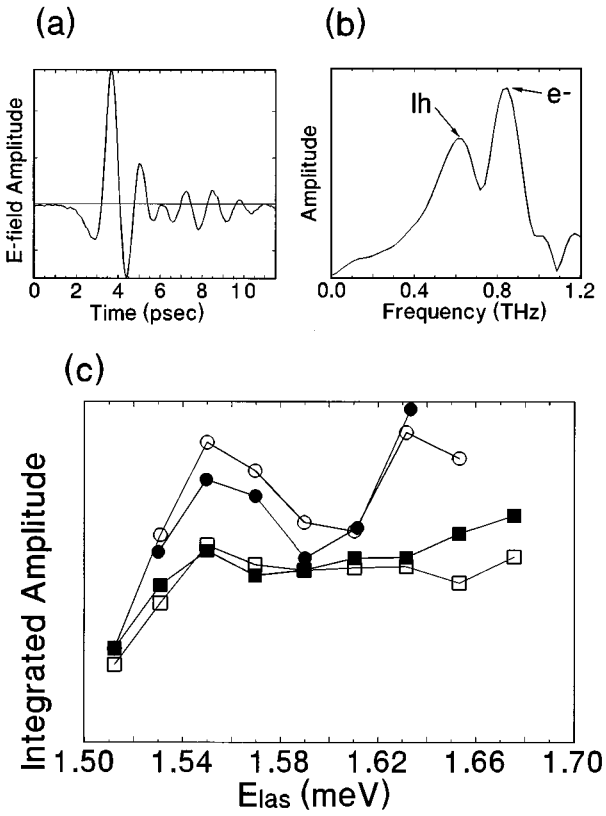

FIG. 2. (a) Time-resolved electric-field oscillations due to photoexcitation cyclotron radiation, $B=2.0$ T, $\lambda=790$ nm, $T=5$ K. (b) Amplitude spectrum of (a); the two peaks correspond to electron (e^-) and light-hole (lh) resonances. (c) Integrated spectral amplitude dependence on laser excitation energy: (●) Voigt, $B=2.0$ T; (○) Voigt, $B=1.5$ T; (■) TF, $B=2.0$ T; (□) TF, $B=1.5$ T; the TF amplitudes are magnified by 2.5×. Note the dip in the Voigt data around the magnetophonon resonance at 1.59–1.61 eV.

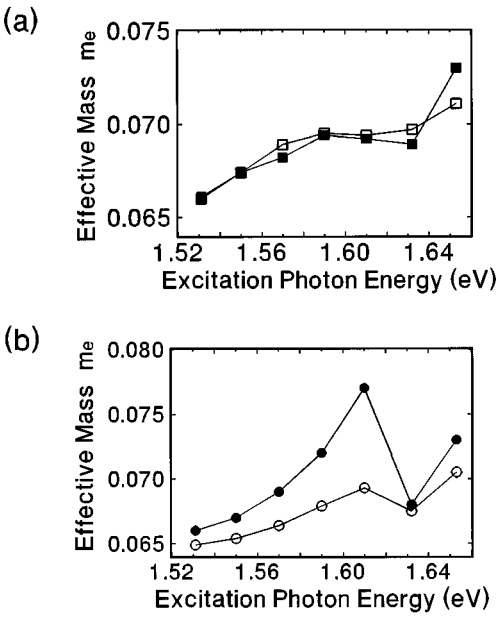

FIG. 3. Electron effective masses as a function of excitation energy, derived from the spectral data. (a) TF geometry (■) $B=2.0$ T; (□) $B=1.5$ T (b) Voigt geometry; (●) $B=2.0$ T; (○) $B=1.5$ T. Whereas the effective-mass peaks near the magnetopolaron resonance in the Voigt configuration, it levels off in the TF case.

The conclusions we may derive from Figs. 2 and 3 coincide nicely with the conceptual picture painted above covering the origin of the coherent cyclotron emission. Two physical mechanisms contribute: ballistic motion of free carriers under the influence of oblique magnetic and electric fields, and the coherent, virtual polarizations induced in the Landau-quantized medium subject to a symmetry-breaking depletion field. Emission from the former is quenched almost entirely in the TF configuration, due to rapid dephasing in the wake of acceleration by the component of E_s parallel to B and subsequent LO-phonon emission. Therefore the magnetophonon resonance at $\hbar\omega=1.59$ eV will not affect the amplitude of the radiation since it does not couple strongly to the virtual excitations; in fact, no decrease is found in the emission at 1.59 eV. The THz radiation in the Voigt geometry, on the other hand, contains contributions from both sources, real and virtual, as is apparent in the larger total signal. At the magnetophonon resonance, the real electrons lose their mutual phase coherence upon scattering to the $n=0$ Landau level. Consequently, that portion of the integrated amplitude is lost and the remaining signal is comparable to that of the TF geometry after correction for the geometric angle factor. The position of the dip, roughly 70–90 meV above the band gap, is consistent with the energy range required to simultaneously excite an electron and a light hole with equal Landau indices (in accord with the magnetooptical selection rules) and with either one of these placed 1 LO-phonon energy (37 meV) from the corresponding $n=0$ Landau level. As noted in Ref. 9 (and references therein), primarily the light-hole excitation is present in magnetoluminescence, and such is the case for THz cyclotron emission [Fig. 2(b)].

The ballistic signal source is regained in the Voigt experiment when the excitation energy passes the resonant coupling point. However, the effective mass changes around 1.61 eV suggest that another resonant process is coming into play: the magnetopolaron. As shown by Lindemann *et al.* for the case of GaAs,[11] an anticrossing occurs in the Landau-level fan plots when the energy of the nth Landau level approaches the energy corresponding to that of a polaron consisting of one LO phonon interacting with an electron in the $n=0$ Landau level. In this conjecture, the possible excitation sequences are as follows: (1) an electron placed high in the lower magnetopolaron branch (which has single-electron character) may dephase via LO-phonon emission, leading to a loss of coherent THz emission; (2) a somewhat higher photon energy will excite the upper magnetopolaron branch (which has more of the polaron character and thus a larger effective mass) and therefore be inhibited from inelastic decay since it already consists of an electron at the $n=0$ Landau level coupled with a phonon; and (3) at yet higher energies, the upper magnetopolaron branch recovers a cyclotronlike behavior, which reduces the cyclotron mass to a value closer to that below the resonance. The magnetopolaron interaction strength increases with magnetic field, hence the larger effective-mass peak for $B=2.0$ T. Strik-

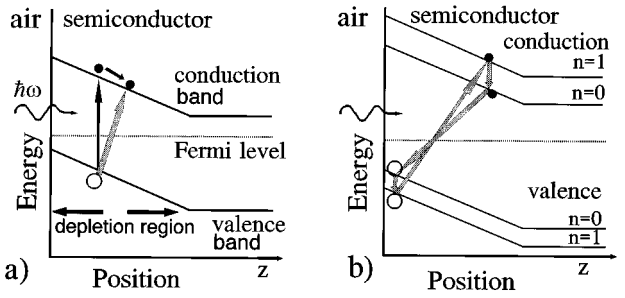

FIG. 4. Photoexcitation processes resulting in THz emission near a semiconductor surface. (a) $B=0$; the solid arrows represent real carrier generation and subsequent acceleration under the surface field, while the cross-hatched arrow illustrates the spatially nonvertical virtual excitations responsible for optical rectification. After Ref. 4. (b) $B\neq 0$; the spatially indirect virtual transitions which generate coherent inter-Landau-level polarizations radiating at the electron and hole cyclotron frequencies.

ingly, the ''plateau'' in the TF effective-mass dispersion around 1.59–1.63 eV may also be interpreted as a consequence of the splitting between the upper and lower magnetopolaron branches. Recalling that the THz radiation due to virtual polarizations results from oscillations between adjacent energy levels, we deduce that photoexcitation spanning the resonance will result in radiation at a higher frequency corresponding to the larger energy separation across the magnetopolaron gap, compared to the usual inter-Landau-level spacing. This frequency, in turn, is translated to an effective mass via $m^*=eB/\omega_c$, leading to a lower value for that component of the THz emission generated by the transient polarizations.

While a rigorous theory for THz generation in magnetic fields has not yet been constructed, we would like to propose a broad framework for calculating the radiation due to coherent, transient polarizations in an electric-field–biased Landau-quantized system. In analogy to the work by Chuang *et al.*[4] for the case of $B=0$, a mixing process is envisioned in which spatially nonvertical photoexcitations take place in the presence of the surface depletion field, resulting in an instantaneous polarization as depicted in Fig. 4(a). In the presence of a finite B field we need to account for the effect of both the conduction- and valence-band magnetically quantized states, as both of these are simultaneously involved and necessary due to the nature of magneto-optical transitions. In our outline for a model, we assume the rules for magneto-optical transitions between simple nondegenerate bands, i.e., $\Delta n=0$ for interband transitions and $\Delta n=\pm 1$ for intraband transitions; and ignore spin splitting as well as the additional complications that arise from LO-phonon interactions and strongly impact the experiment. We then find that the expression for the nonlinear susceptibility found in Eq. (2) of Ref. 4 should take on the form

$$\chi^{(n.l.)}(\omega_c^e,\omega_c^h;-\omega,\omega+\omega_c^e+\omega_c^h)$$
$$=-\frac{1}{V}\sum_{pqns}\frac{\mu_{pnqn}}{\epsilon_{epn}+\epsilon_{hqn}-\omega-\omega_c^e-\omega_c^h-i/\tau}$$
$$\times\sum_{n',m'}\frac{\langle p'n-1|ez_e|pn\rangle\langle qn|ez_h|q'n-1\rangle\mu^*_{p'n-1q'n-1}}{\epsilon_{ep'n-1}+\epsilon_{hq'n-1}+\omega+i/\tau}$$
$$+\ \text{permutations}. \qquad (3)$$

Here $\hbar=1$, V is the crystal volume, τ the dephasing time, s the spin quantum number, n the Landau-level index, p and q the electron and hole eigenstates perpendicular to the magnetic field (rather than perpendicular to the surface, as in Ref. 4); $\langle p'n-1|ez_e|pn\rangle$ and μ_{pnqn} are the inter-Landau-level and interband dipole matrix elements. Figure 4(b) illustrates the transitions involved in this interaction in a highly simplified schematic, near the band gap. As shown in the figure, above-band photoexcitation produces a *double* macroscopic polarization at the electron and hole cyclotron frequencies, in contrast to the standard nonlinear susceptibilities which describe only one output wave.

In conclusion, we have demonstrated the ability to discriminate between the contributions of two mechanisms to the generation of photoexcited transient cyclotron emission in bulk GaAs: ballistic motion of real carriers, and surface-field-enhanced, coherent inter-Landau-level polarizations. These are differentiated by a combination of magnetic-field orientation and excitation wavelength. While these results are important for understanding the photoexcited THz radiation from other systems, a firm theoretical foundation is still lacking for quantitative interpretations.

This work has been supported by National Science Foundation Grants Nos. DMR-9112329 and DMR-9121747. D.S. has also been supported in part by Los Alamos National Laboratory.

*Present address: Los Alamos National Laboratory, Group MST-11, MS E525, Los Alamos, NM 87545. Electronic address: dansome@lanl.gov

[1] X.-C. Zhang and D.H. Auston, J. Appl. Phys. **71**, 326 (1992).
[2] B.B. Hu, A.S. Weling, D.H. Auston, A.V. Kuznetsov, and C.J. Stanton, Phys. Rev. B **49**, 2234 (1994).
[3] P.N. Saeta, B.I. Greene, and S.L. Chuang, Appl. Phys. Lett. **63**, 3482 (1993).
[4] S.L. Chuang, S. Schmitt-Rink, B.I. Greene, P.N. Saeta, and A.F.J. Levi, Phys. Rev. Lett. **68**, 102 (1992).
[5] B.I. Greene, P.N. Saeta, D.R. Dykaar, S. Schmitt-Rink, and S.L. Chuang, IEEE J. Quantum Electron. **28**, 2302 (1992).
[6] X.-C. Zhang, Y. Jin, K. Ying, and L.J. Schowalter, Phys. Rev. Lett. **69**, 2303 (1992).
[7] B.B. Hu, E.A. de Souza, W.H. Knox, J.E. Cunningham, M.C. Nuss, A.V. Kuznetsov, and S.L. Chuang, Phys. Rev. Lett. **74**, 1689 (1995).
[8] D. Some and A.V. Nurmikko, Phys. Rev. B **50**, 5783 (1994).
[9] S.I. Gubarev, T. Ruf, M. Cardona, and K. Ploog, Phys. Rev. B **48**, 1647 (1993).
[10] T. Takagahara, in *Relaxation of Elementary Excitations*, edited by R. Kubo and E. Hanamura, Solid State Sciences Vol. 18 (Springer-Verlag, New York, 1980), p. 45; N. Pelekanos, J. Ding, Q. Fu, A.V. Nurmikko, S.M. Durbin, M. Kobayashi, and R.L. Gunshor, Phys. Rev. B **43**, 9354 (1991).
[11] G. Lindemann, R. Lassnig, W. Seidenbusch, and E. Gornik, Phys. Rev. B **28**, 4693 (1983).